GSA Data Repository 2016090

Very long-term stability of passive margin escarpment constrained by $^{40}Ar/^{39}Ar$ dating of K-Mn oxides,

DOI:10.1130/G37303.1.

Anicet Beauvais et al.

Supplementary material

Manganiferous ore samples have been sampled in upland Sandur ore deposits (KPA-8: 15° 0' 2.27"N/76° 32' 41.6"E; KMK-2: 14° 59' 48.34"N/76° 34' 40.34"E) and in lowland ore deposits, Naveli (NAV-3: 15° 07' 55.10"N/74° 09' 49.72''E; NAV-4: 15° 08' 07.12"N/74° 09' 32.26''E), and Caurem (CAU-1: 15° 07' 2.19"N/74° 08' 39.66"E; CAU-3: 15° 07' 3.47"N/74° 08' 38.97"E). Samples were collected on benches in mining pits (Figure DR1).

1. Characterization of samples

The method implemented to characterize and separate cryptomelane grains from field samples is summarized as follow (see also Bonnet et al. 2014). Field samples were cut with a circular saw (1.5 mm breadth) to get a good section allowing accurate observations. A 200-300 µm thick polished thin section and a symmetrical 500 µm thick slab were made from each sawed fragment. Polished thin sections have been studied using reflected light microscopy. We also performed elemental cartography by X-ray micro-fluorescence (µ-XRF) with a XGT7000 Horiba Jobin Yvon producing a high-intensity beam with a 100 µm spot size, Rh X-ray tube, accelerating voltage of 30 kV and current of 1mA. Micro-XRF elemental maps of Fe, K and Mn are stacked together on a single image using ImageJ software by assigning a distinct color to each elemental map (Figure DR2). The resulting images are

helpful to localized cryptomelane phases on the slab. Electron Probe Micro-chemical Analysis (EPMA) of minerals using a CAMECA SX-100 electron microprobe equipped with five wavelength-dispersive X-ray spectrometers (WDS) provided an accurate micro chemical composition of cryptomelane (Table DR1).

Cryptomelane grains were then separated from the 300-500 μm thick slabs slabs using a micro-drill under a large magnifier. Some of them were observed with a scanning electron microscope (SEM) (Figure DR2), other were crushed to produce a powder sieved at 64 μm, which was analyzed by XRD using a Panalytical X'Pert Pro MPD with a Co Kα X-ray source (λ = 1.79 Å) operating at 40kV and 40 mA (see Figure DR3).

2. Dating of cryptomelane grains

The separated cryptomelane grains were selected by hand picking and ultrasonically cleaned in absolute ethanol and conditioned in aluminium foil packets, to be irradiated for 50 hours in the TRIGA Mark-II reactor of Pavia University (Italia). Prior experiments have shown none or very little ^{39}Ar recoil from those cryptomelane grains. The Factor J was determined from the analysis of the standard Taylor Creek Rhyolite sanidine-2 (TCRs-2) monitor, with an age of 28.608 ± 0.033 Ma (Renne et al., 2011). The standard was analyzed after every ten unknown samples. After a two-month "cooling" period, the irradiated cryptomelane grains were analyzed using either step heating degassing under a CO2 laser probe coupled with an Argus VI multi-collection mass spectrometer (with 4 faradays for masses 40Ar-37Ar and ion counting on 36Ar) or a step-wise heating procedure in a double vacuum Staudacher-type furnace coupled with a VG3600 mass spectrometer using peak jumping and Faraday/Daly analyzer as described by Arnaud et al. (2003). The furnace temperature was calibrated by means of a classical thermocouple, and the gas purification was accomplished using a cold trap with liquid air and Al–Zr AP10 getters (one hot, one cold) for

8 minutes before the introduction into the VG3600 mass spectrometer. One minute was allowed for equilibration before analysis. ^{40}Ar and ^{39}Ar were measured on a Faraday cup with a resistor of 10^{11} ohm, while ^{39}Ar, ^{38}Ar, ^{37}Ar, and ^{36}Ar were analyzed using a scintillator and photomultiplier after interaction on a Daly plate. Mass discrimination of machines is followed daily, such as blank levels. Isotopic ratios were corrected for irradiation interferences and air contamination using a mean air value $(^{40}Ar/^{36}Ar)_{atm}$ of 298.56 ± 0.31 (Lee et al., 2006; Renne et al., 2009). The analytical data are reported in data repositories (Tables DR2 and DR3), and the errors are quoted at the 1σ level. Ages are statistically analyzed in two ways: ^{39}Ar release spectra and inverse isochrones (Figure DR4). Plateau ages are calculated from at least three consecutive ^{39}Ar release steps comprising up to 50% of total $^{39}Ar_K$ released and overlapping at the 2σ confidence level (Fleck et al., 1977). Isochrone ages are accepted when mean square weighted deviation (MSWD) is less than 2.5 and the $^{40}Ar/^{36}Ar$ intercept within 2σ from the $(^{40}Ar/^{36}Ar)_{atm}$ value.

3. References cited

Arnaud, N., Tapponier, P., Roger, F., Brunel, M., Scharer, U., Wen, C., and Xu, Z., 2003, Evidence for Mesozoic shear along the western Kunlun and Altyn-Tagh fault, northern Tibet (China) : Journal of Geophysical Research, v. 108, doi:10.1029/2001JB000904

Bonnet, N.J., Beauvais, A., Arnaud, N., Chardon, D., Jayananda, M., 2014. First $^{40}Ar/^{39}Ar$ dating of intense Late Palaeogene lateritic weathering in Peninsular India. Earth Planet. Sci. Lett. 386, 126–137. doi:10.1016/j.epsl.2013.11.002

Fleck, R.J., Sutter, J.F., and Elliot, D.H., 1977, Interpretation of discordant $^{40}Ar/^{39}Ar$ age-spectra of mesozoic tholeiites from Antarctica: Geochimica et Cosmochimica Acta, v. 41, p. 15-32.

Lee J-Y, Marti, K., Severinghaus, J.P., Kawamura, K., Yoo, H.S., Lee, J.B., and Kim, J.S., 2006, A redetermination of the isotopic abundances of atmospheric Ar: Geochimica et Cosmochimica Acta, v. 70, p. 4507–4512.

Renne, P.R., Balco, G., Ludwig, K.R., Mundil, R., and Min, K., 2011, Response to the comment by W.H. Schwarz et al. on "Joint determination of ^{40}K decay constants and ^{40}Ar•/^{40}K for the Fish Canyon sanidine standard, and improved accuracy for ^{40}Ar/^{39}Ar geochronology" by P.R. Renne et al. (2010): Geochimica et Cosmochimica Acta, v. 75, p. 5097–5100. doi:10.1016/j.gca.2011.06.021

Renne, P.R., Cassata, W.S., and Morgan, L.E., 2009, The isotopic composition of atmospheric argon and 40Ar/39Ar geochronology: time for a change: Quaternary Geochronology, v. 4, p. 288-298.

FIGURE DR1

Figure DR1. Location of samples collected in the different Mn ore deposits and lateritic weathering profiles. **(a)** KPA-8, and **(b)** KMK-2, in the highland Sandur Mn ore deposits; **(c)** CAU-3, and **(d)** NAV-3, in the coastal lowland lateritic weathering profiles. White crosses indicate the sampling spots. The white contour line delimits Mn rich ore pockets.

HIGHLAND

ⓐ KPA-8

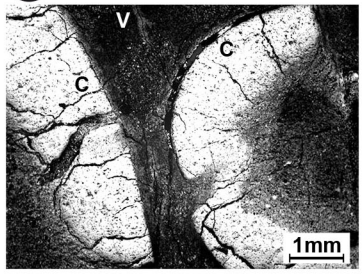

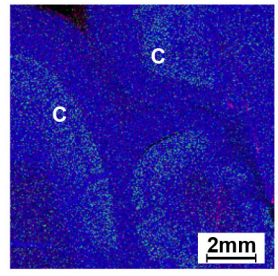

ⓑ KMK-2

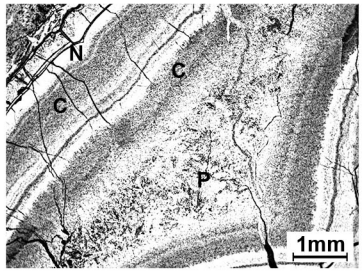

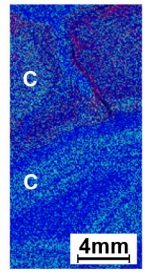

LOWLAND

ⓒ CAU-3

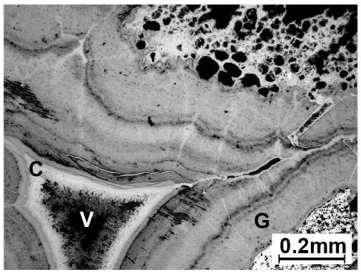

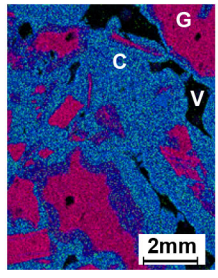

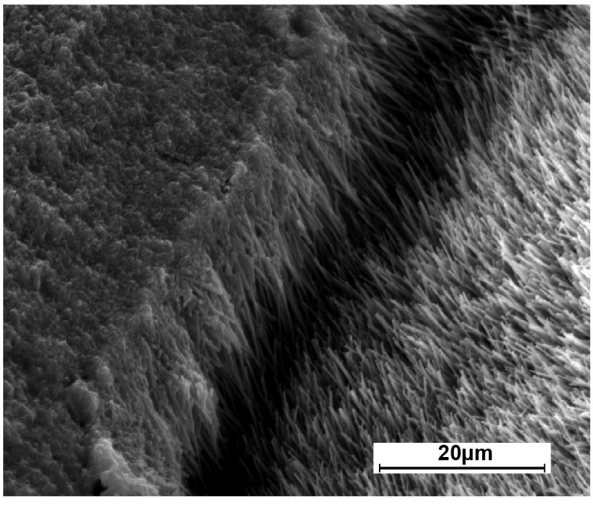

ⓓ NAV-3

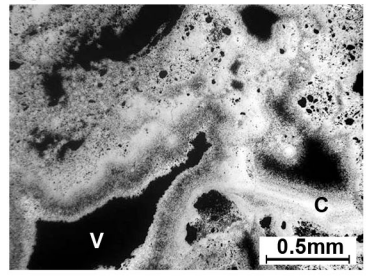

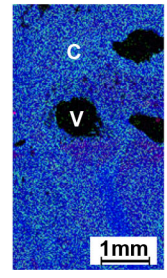

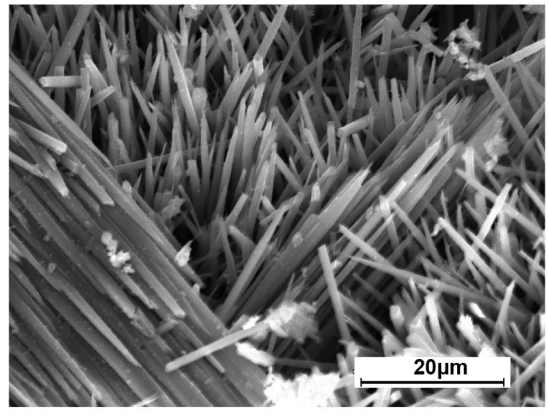

FIGURE DR2

Figure DR2. Mineralogical characterization of samples combining reflected-light photomicrography, μ-XRF mapping, and SEM imaging to precisely identify cryptomelane. **(a)** KPA-8, and **(b)** KMK-2 from the Sandur profile in the highland; **(c)** NAV-3, and **(d)** CAU-3 from the Mn lateritic weathering profiles in the lowland**.** The μ-XRF map yields the composite colored image with Mn in blue, Fe in red and K in green allowing to precisely identifying cryptomelane. C = Cryptomelane; P = Pyrolusite; N = Nsutite; G = Goethite V= void.

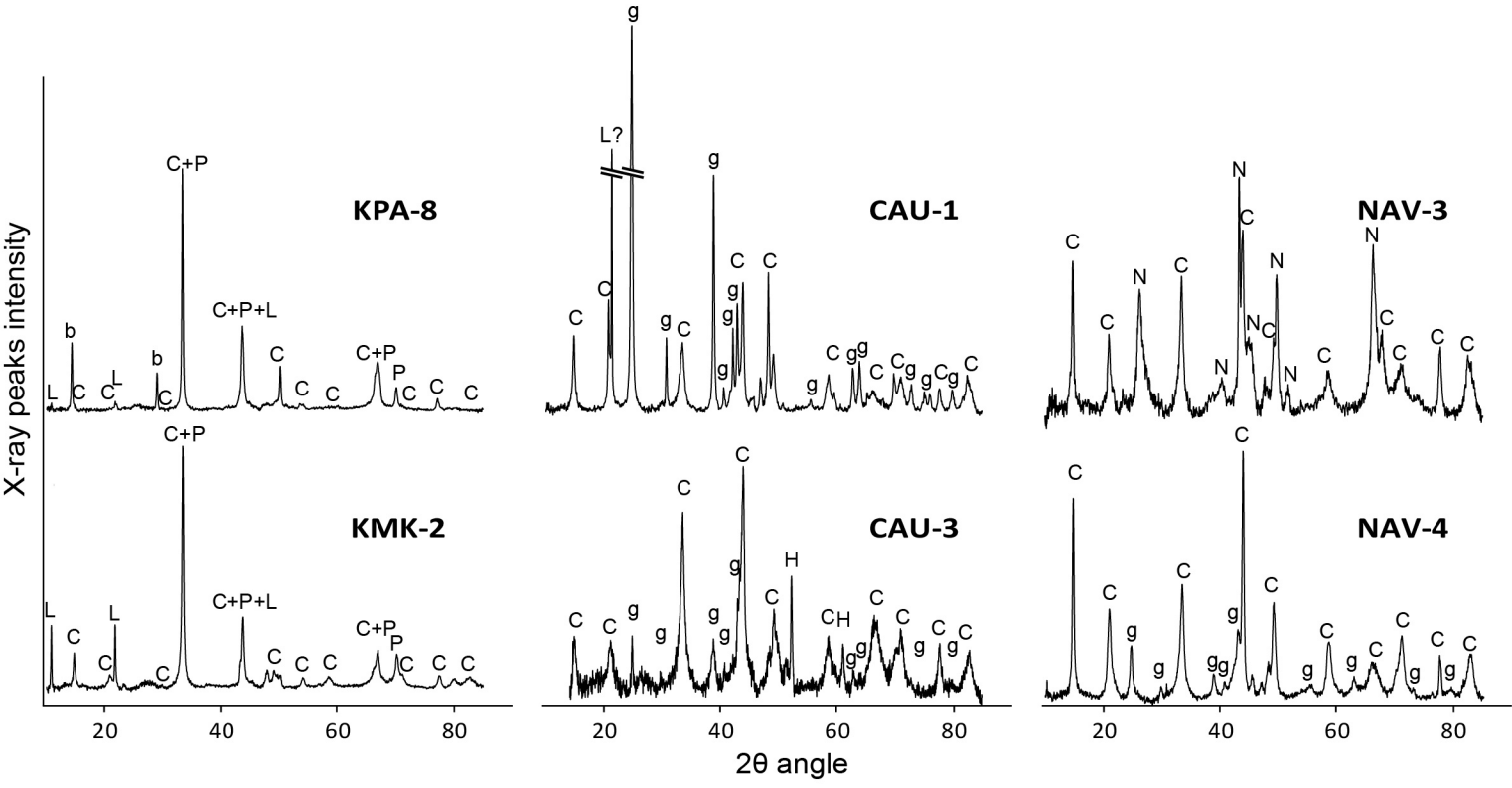
KPA-8
KMK-2
CAU-1
CAU-3
NAV-3
NAV-4
X-ray peaks intensity
2θ angle
20
40
60
80

FIGURE DR3

Figure DR3. Mineralogical Characterization of samples using X-Ray diffraction. C = Cryptomelane; P = Pyrolusite; b = birnessite ; L = lithiophorite ; N = nsutite ; g = Goethite; H = Hollandite.

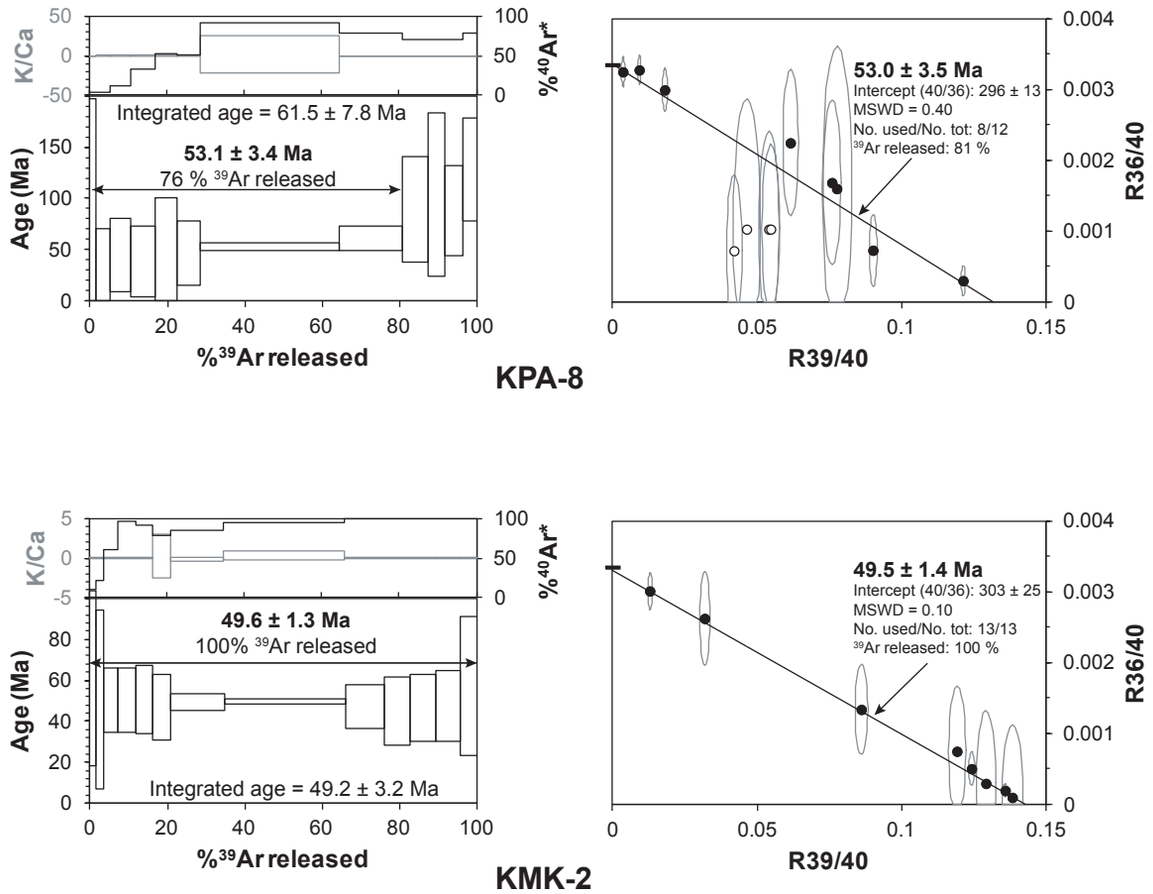
K/Ca
%40Ar*
Integrated age = 61.5 ± 7.8 Ma
53.1 ± 3.4 Ma
76 % 39Ar released
Age (Ma)
%39Ar released
53.0 ± 3.5 Ma
Intercept (40/36): 296 ± 13
MSWD = 0.40
No. used/No. tot: 8/12
39Ar released: 81 %
R36/40
R39/40
KPA-8
49.6 ± 1.3 Ma
100% 39Ar released
Integrated age = 49.2 ± 3.2 Ma
49.5 ± 1.4 Ma
Intercept (40/36): 303 ± 25
MSWD = 0.10
No. used/No. tot: 13/13
39Ar released: 100 %
KMK-2

Figure. DR4- A

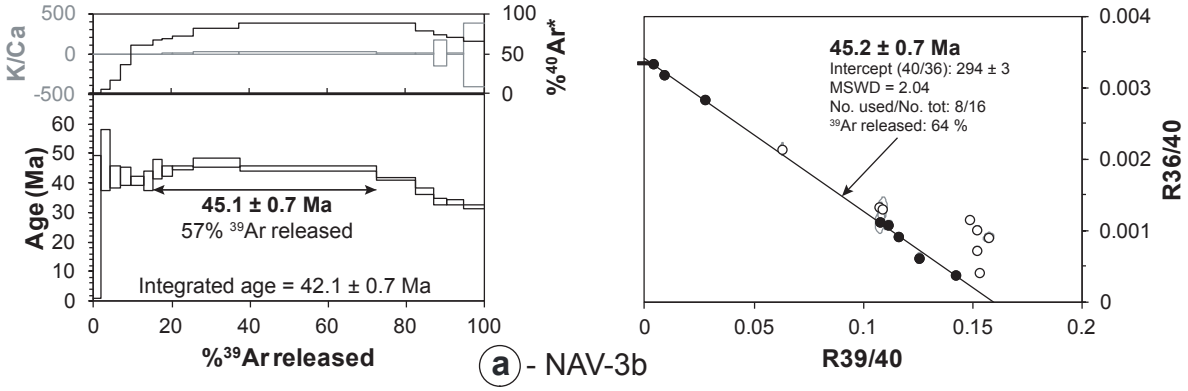

(a) - NAV-3b

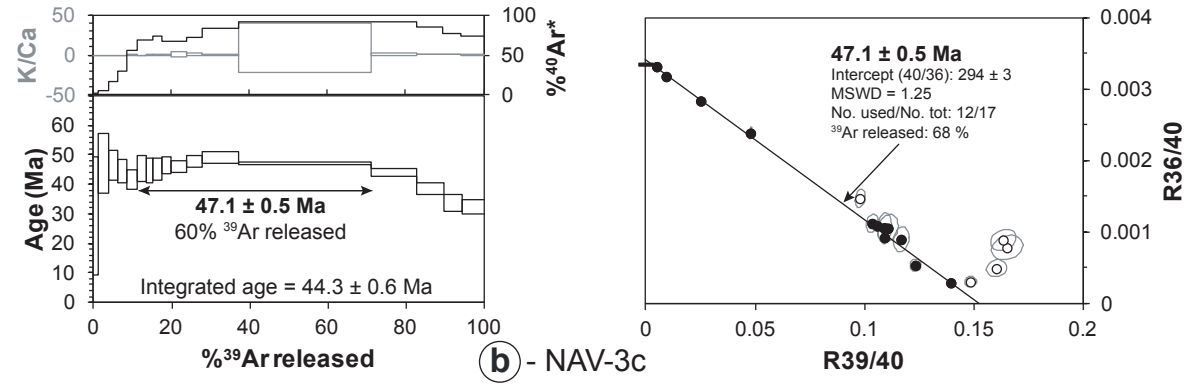

(b) - NAV-3c

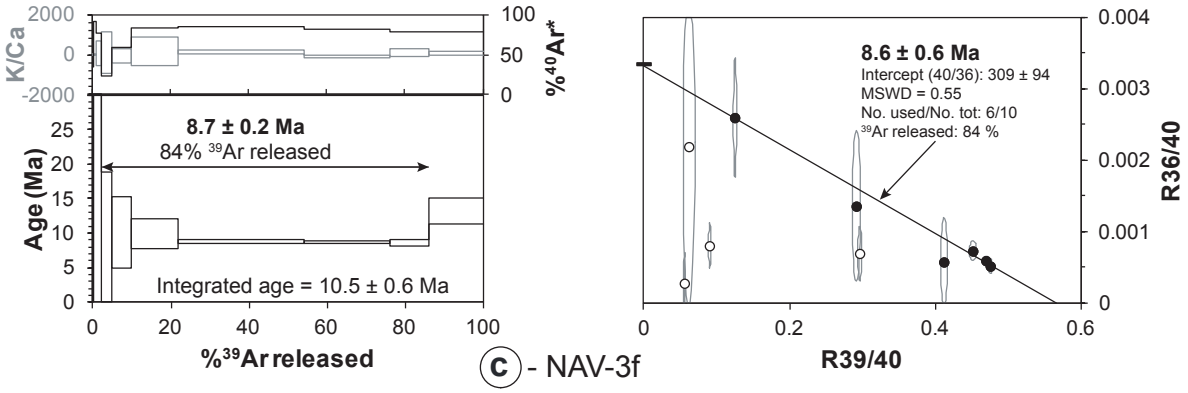

(c) - NAV-3f

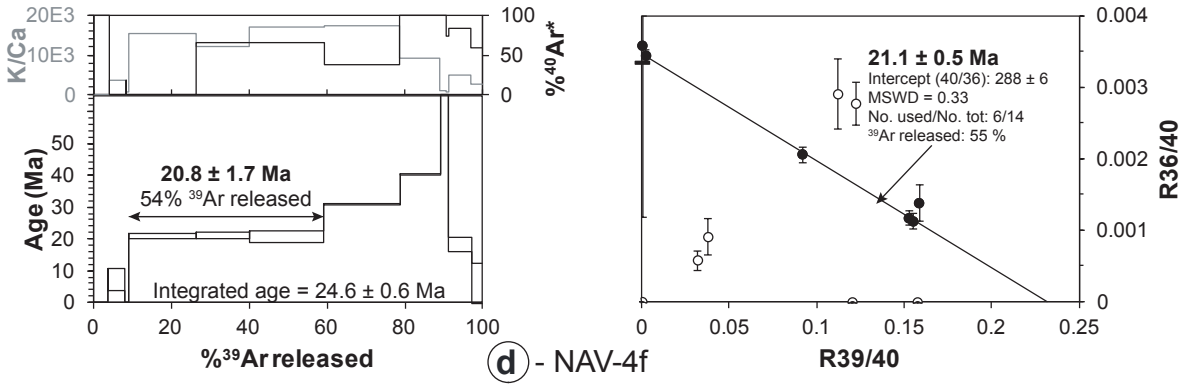

(d) - NAV-4f

FIGURE. DR4-B

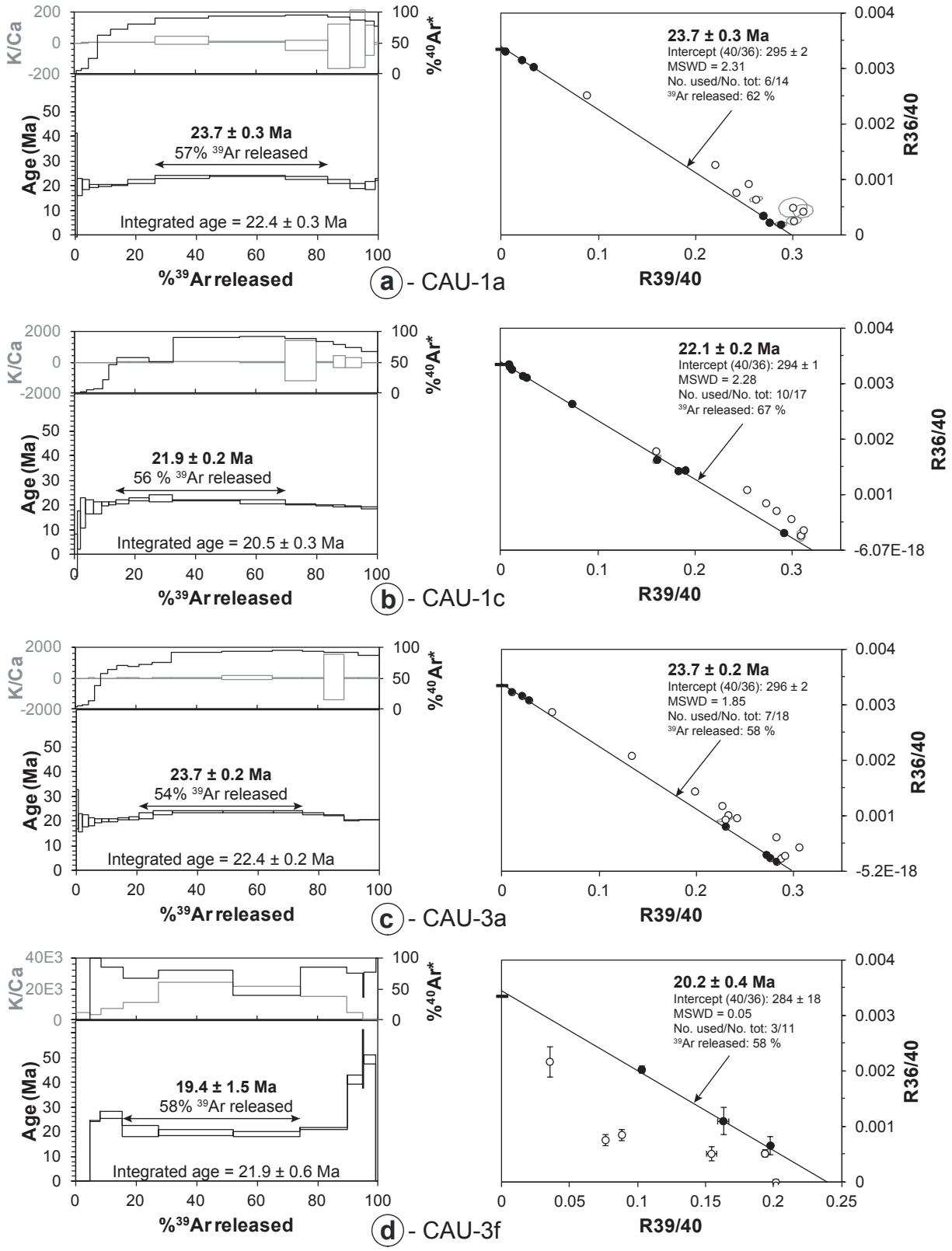
K/Ca
%40Ar*
Age (Ma)
23.7 ± 0.3 Ma
57% 39Ar released
Integrated age = 22.4 ± 0.3 Ma
%39Ar released
23.7 ± 0.3 Ma
Intercept (40/36): 295 ± 2
MSWD = 2.31
No. used/No. tot: 6/14
39Ar released: 62 %
R36/40
R39/40
a - CAU-1a
21.9 ± 0.2 Ma
56 % 39Ar released
Integrated age = 20.5 ± 0.3 Ma
22.1 ± 0.2 Ma
Intercept (40/36): 294 ± 1
MSWD = 2.28
No. used/No. tot: 10/17
39Ar released: 67 %
-6.07E-18
b - CAU-1c
23.7 ± 0.2 Ma
54% 39Ar released
Integrated age = 22.4 ± 0.2 Ma
23.7 ± 0.2 Ma
Intercept (40/36): 296 ± 2
MSWD = 1.85
No. used/No. tot: 7/18
39Ar released: 58 %
-5.2E-18
c - CAU-3a
19.4 ± 1.5 Ma
58% 39Ar released
Integrated age = 21.9 ± 0.6 Ma
20.2 ± 0.4 Ma
Intercept (40/36): 284 ± 18
MSWD = 0.05
No. used/No. tot: 3/11
39Ar released: 58 %
d - CAU-3f

FIGURE. DR4-C

Figure DR4. ^{39}Ar releasing spectra showing well defined plateau ages with K/Ca (grey) and Ar* (black) step curves (left) and inverse isochrone diagrams (right) of cryptomelane grains from the open pits samples of **(A)** Sandur **(B)** Naveli and **(C)** Caurem Mn ore deposits (MSWD = mean square weighted deviation).

Table DR1. Electron microprobe analyses (EPMA) of cryptomelane spots in polished thin sections.

Table DR2 and Table DR3. Analytical results obtained for highland and lowland cryptomelane grains, either from Laser energy (spectrometer Argus IV) or double vacuum Staudacher-type furnace temperature, T °C, (spectrometer VG 3600) for each irradiated crypromelane grain. The concentrations of ^{36}Ar, ^{37}Ar, ^{38}Ar, ^{39}Ar and ^{40}Ar with their respective 1σ error are provided for each step heating. The amount of $^{40}Ar^*$ (%), of ^{39}Ar released (%^{39}Ar) and the K/Ca ratio (derived from $^{39}Ar/^{37}Ar$) are also given. Finally, this table show ratios $^{40}Ar^*/^{39}Ar_k$ used to determine the corresponding apparent ages, which are presented in the last column with their associated 2σ error. The different J-Factor values are also provided for each irradiated grains. The sensitivity of VG 3600 is 1E-17 mol/mV and 1E-3 Amps/Torr on Argus IV spectrometer.